

# Melanoma-Derived Exosomes Endow Fibroblasts with an Invasive Potential via miR-21 Target Signaling Pathway

This article was published in the following Dove Press journal:  
*Cancer Management and Research*

Chenmeiyi Wang<sup>1,2,\*</sup>  
Yiting Wang<sup>1,2,\*</sup>  
Xiulin Chang<sup>1,2</sup>  
Xiaoyun Ba<sup>1,2</sup>  
Na Hu<sup>1,2</sup>  
Qing Liu<sup>1,2</sup>  
Liaoqiong Fang<sup>1,2</sup>  
Zhibiao Wang<sup>1,2</sup>

<sup>1</sup>State Key Laboratory of Ultrasound Engineering in Medicine, College of Biomedical Engineering, Chongqing Medical University, Chongqing 400016, People's Republic of China; <sup>2</sup>National Engineering Research Center of Ultrasound Medicine, Chongqing 401121, People's Republic of China

\*These authors contributed equally to this work

**Background:** Tumor-derived exosomes are messengers that participate in tumor progression. Fibroblasts are associated with the metastasis of cancer depending on their cellular plasticity. We hypothesize that tumor-derived exosomes endow the fibroblasts in tumor microenvironment with invasive phenotype to the benefit of tumor metastasis.

**Materials and Methods:** Exosomes derived from B16-F10 cells were identified by nanoparticle tracking analyzer (NTA), dynamic light scattering (DLS), Western blot (WB), and transmission electron microscopy (TEM). Cell invasion and migration assays were performed using the xCELLigence real-time cell analyzer (RTCA). Role of tumor-derived exosomal miR-21 in cell invasion was determined by qPCR.

**Results:** The invasion analysis showed that exosome-treated fibroblast cells had greater invasive capability as compared to untreated fibroblast cells, with the higher expressions of MMP2 and MMP9. miR-21 is at least partially responsible for this effect. After ingestion of melanoma-derived exosomes during incubation, mouse embryonic fibroblasts cells emerged cellular invasiveness with the presentation of a marked increase in miR-21 expression. MiR-21 promoted invasion of fibroblasts by down-regulation of tissue inhibitor of metalloproteinase 3 (TIMP3) expression and increasing of matrix metalloprotein (MMP) expression in fibroblast cells via melanoma-derived exosomes in a time-dependent manner.

**Conclusion:** Our results suggest that tumor-derived exosomes may facilitate stromal fibroblasts an aggressive phenotype to equip the tumor progression.

**Keywords:** melanoma, exosomes, miR-21

## Introduction

Exosomes are small membrane vesicles of endocytic origin that are released into the extracellular compartment upon fusion of multivesicular bodies (MVB) with the plasma membrane.<sup>1</sup> It has been found that exosomes can mediate local and systemic cell communication with transmitting signals from one cell to another on the molecular level.<sup>2,3</sup> Tumor cell-derived exosomes carry particular molecular components originated from donor cells to mediate tumorigenesis and drive tumor progression by regulating tumor microenvironment. So tumor cells-derived exosomes. Many data have demonstrated that tumor exosomes are emerging mediators of tumorigenesis.<sup>4-6</sup>

It is confirmed that large variety of miRNAs in exosomes play important roles in tumor metastasis and invasion.<sup>7</sup> It has been shown that miR-21 is a promoter of oncogenes and is highly expressed in several malignant tumors.<sup>8,9</sup> The high-invasion

Correspondence: Zhibiao Wang;  
Liaoqiong Fang  
Tel/Fax +0086-023-68485021  
Email wangzb@cqmu.edu.cn;  
lqfang06@163.com

and metastatic tendency of melanoma tumors complicates treatment of the malignancy. Studies have shown that miR-21 can promote invasion of melanoma cells.<sup>10</sup> High expression of miR-21 in melanoma cells inhibits mRNA expression of crucial tumor suppressor proteins such as the tissue inhibitor of metalloproteinases 3 (TIMP3).<sup>11</sup> This results in increased matrix metalloproteinase activity, playing a pivotal role in the process of invasion and metastasis.

Studies have shown that tumor cells can “cross-talk” with surrounding cells through exosomes released in the extracellular compartment to promote tumor invasion and metastasis.<sup>12</sup> Fibroblasts surrounding tumors can play a significant role in tumor progression.<sup>13,14</sup> When melanoma cells are cultured on feeder fibroblasts treated with melanoma-derived exosomes, the melanoma cells exhibit more invasive and metastatic properties.<sup>12</sup> However, only limited information is available regarding the effect of tumor exosomes on mesenchymal cells.

Therefore, we asked if we use exosomes derived from highly invasive melanoma cells containing miR-21 to directly treat fibroblasts, would the fibroblast phenotype be altered? Mouse melanoma B16-F10 cells and the homologous mouse embryonic fibroblast (MEF) cells were used in this study. We studied the effect of B16-F10 cell-derived exosomes on the invasion ability of fibroblast cells and the role of oncogene miR-21 in this process. Our data indicate that exosomes derived from highly invasive tumor cells act as messengers that participate in altering the invasive phenotype of cells at the periphery of the tumor. This may be an important novel aspect in understanding tumor invasion and metastasis.

## Materials and Methods

### Reagents

Dulbecco’s modified Eagle’s medium (DMEM), RPMI and fetal bovine serum (FBS) were purchased from Hyclone. MMP2, MMP9 and E-cadherin antibodies were obtained from abcam. BCA protein assay kit was purchased from Beyotime. 5(6)-Carboxy fluorescein diacetate N-succinimidyl ester (CFSE) was obtained from Sigma.

### Cell Culture

All animal experiments were conducted at The Chongqing Medical University and were approved by The Ethics Committee of Chongqing Medical University. All experimental protocols were performed according to the Guidelines for the Care and Use of Laboratory Animals.

Mouse embryonic fibroblast (MEF) cells from Day 13.5 embryos were collected using standard methods and then cultured in Dulbecco’s modified Eagle’s medium (DMEM) supplemented with 10% (v/v) fetal bovine serum (FBS), 50 U/mL penicillin and 50 µg/mL streptomycin. Cells were grown as proliferative (1 day-culture) or quiescent (confluent and 24 h serum-starved) cultures.

B16-F10 cell lines were acquired from the China Cell Bank. B16-F10 cells were maintained in RPMI supplemented with 10% FBS. The cells were cultivated routinely at 37°C in 5% CO<sub>2</sub>. Once the fibroblasts reached 80% cell confluence, the fibroblasts were co-cultured with exosomes derived from B16-F10 cells for 48 h. The fibroblasts were then harvested for analysis.

### Isolation of Exosomes

The isolation of exosomes derived from B16-F10 cells was performed following the protocol developed in a previously published study.<sup>17</sup> Briefly, cells were cultured in media supplemented with 10% exosome-depleted FBS (FBS, Hyclone). FBS was depleted of bovine exosomes by ultracentrifugation at 100,000×g for 70 min. Exosomes were purified from cell culture supernatants by a combination of ultracentrifugation and filtration. First, culture medium was collected and centrifuged at 400×g for 5 min to remove whole cells. The supernatant was then centrifuged at 2000×g for 15 min to remove debris. The supernatant was then centrifuged at 5000×g for 15 min to remove debris. The supernatant was then centrifuged at 10,000×g for 30 min to remove debris. Exosomes were then harvested by centrifugation at 100,000×g for 70 min. The pellet was resuspended and washed twice with PBS.

### NanoSight Nanoparticle Tracking Analyzer (NTA)

The nanoparticle tracking analysis of the exosomes was performed using a NanoSight NS300 instrument (Malvern Instruments, Worcestershire, UK) calibrated with 100-nm polystyrene beads (Polysciences, Warrington, PA). Particle suspensions were diluted in PBS to a concentration of 1–8×10<sup>8</sup> particles/mL for the nanoparticle tracking analysis. The Stokes–Einstein equation was employed to determine the size distribution and number of particles (concentration) within the sample.

### Dynamic Light Scattering

Twenty micrograms of exosomes were dissolved in sterile PBS to a total volume of 1 mL, then aspirated into an

insulin syringe and loaded into the sample chamber. The exosomes size and distribution were measured in Zetasizer Nano ZS apparatus (Malvern Instruments, Worcestershire, UK) equipped with laser of  $\lambda = 633$  nm.

## Transmission Electron Microscopy

The exosomes pellet was perfused in 4% glutaraldehyde, fixed for 2 h, cleaned via 3 rinses of PBS, fixed in 1% osmium tetroxide for 2 h, dehydrated by ethanol and acetone, soaked in epoxy resin, embedded and polymerized, and cut into sections with thicknesses of 0.5  $\mu\text{m}$ . Ultrathin sections with thicknesses of 60 nm were fixed and prepared under a fluorescent microscope and stained with uranium acetate and lead citrate. Myocardial ultrastructure was observed and photographed using a transmission electron microscope (TEM, H-7500 type, Hitachi, Japan) equipped with a digital CCD (Gatan-780, Gatan Inc., USA).

## Invasion Assays

Cell invasion and migration assays were performed using the xCELLigence Real-Time Cell Analyzer (RTCA) DP instrument (Ozyme (Montigny Le Bretonneux, France). The xCELLigence RTCA DP instrument cellular invasion/migration plate (CIM-plate 16) uses micro-electronic sensors on the underside of an 8  $\mu\text{m}$  microporous polyethylene terephthalate (PET) membrane of a Boyden-like upper chamber. Cells migrating from the upper chamber through the membrane interact and adhere to the electronic sensors, thus causing an increase in electrical impedance [41]. Changes in cell impedance over time indicate the change in the number of cells interacting with electrodes, therefore allowing automatic and continuous measurement of migration. For invasion assays, the upper surface of the membrane was incubated at 37°C/5% CO<sup>2</sup> for 4 h, then washed with PBS. For all migration and invasion assays, 160  $\mu\text{L}$  of RPMI media supplemented with 5% FBS was added to the lower chamber of each well and 50  $\mu\text{L}$  of RPMI to the upper chamber and the plate pre-incubated for 1 h at 37°C/5% CO<sup>2</sup>. Cumulus cell migration and invasion was monitored using the RTCA DP instrument, taking cell impedance readings every 10 min for a minimum of 96 h.

## Immunostaining

CFSE was diluted 1:100 in approximately 20  $\mu\text{g}$  of exosomes solution and then incubated at 37°C for 15 min. The mixtures were then washed with excess PBS and redeposited by three cycles of centrifugation (100,000 $\times$ g for 70 min). After co-cultured with labeled exosomes (20  $\mu\text{g}/\text{mL}$ )

for the indicated time, fibroblast cells were observed under a confocal microscope (Nikon Microsystems).

After fibroblast cells were co-cultured with tumor for 48 h and fixed with acetone at 4°C for 15 min. Samples were incubated, respectively, with primary antibodies for 1 h and then incubated with GFP-conjugated rabbit anti-mouse IgG in the dark for 60 min at 37°C. Then, the sections were incubated in 4, 6-diamidino-2-phenylindole (DAPI) at 37°C for 8 min. Next, they were washed with PBS and mounted with 50% glycerol. Fibroblast cells were observed under a confocal microscope. Digital images were recorded and analyzed using NIS 4.2 Viewer and Image Pro Plus software.

## Transfection

The exosomes were transfected with inhibitor-miR-21 (RiboBio, Guangzhou, China) using riboFECTTM CP (RiboBio, Guangzhou, China), according to the manufacturer's instructions.

## RNA Expression Analysis by qPCR

RNA was extracted from fibroblast cells (1 $\times$ 10<sup>6</sup> cells) using TRIzol reagent (Invitrogen Life Technologies) and cDNA was generated via RT. The miRNAs were purified using an All-in-One microRNA extraction kit (GeneCopoeia, Rockville, MD, USA), according to the manufacturer's instructions. qPCR was performed using an ABI StepOne Plus real-time PCR system (Applied Biosystems, Foster City, CA, USA). The primer sequences were as follows: MMP2, forward CCCCATGCTGATACTGA and reverse CTGTCCG CCAAATAAACC; MMP9, forward CTCAAGTGG GACCATCATAACA and reverse GATACCCG TCTCCGTGCT; TIMP3, forward CTTCTGCAACTCCG ACATCGT and reverse GGGGCATCTTACTGAAGCCTC. The relative expression levels of miR-21 were calculated using the 2<sup>- $\Delta\Delta\text{CT}$</sup>  method (14), in which  $\Delta\text{CT}$  was defined as the threshold cycle (CT) value of the U6 internal control minus the CT value of the target miRNA. The expression levels of MMP2, MMP9 and TIMP3 were normalized against GAPDH and calculated using the 2- $\Delta\Delta\text{CT}$  method.

## Western Blot (WB) Analysis

Extracted total proteins were incubated with cold radioimmunoprecipitation (RIPA) lysis buffer and separated by 12% sodium dodecyl sulfate polyacrylamide gel electrophoresis. The proteins were transferred to 0.22  $\mu\text{m}$  polyvinylidene difluoride (PVDF) membranes (Bio-Rad) and reacted with primary antibodies at 4°C overnights. After washing with

Tris-buffered saline containing Tween 20 (TBST), the membranes were incubated with peroxidase-conjugated secondary antibodies. Protein expression was normalized to b-actin expression. Antibodies bound on the membrane were detected using an enhanced chemiluminescence detection system (Millipore) according to the manufacturer's instructions.

## Immunocytochemical Staining

After fibroblast cells were co-cultured with tumor for 48 h and fixed with acetone at 4°C for 15 min. Samples were incubated, respectively, with primary antibodies for 1 h and then incubated with GFP-conjugated rabbit anti-mouse IgG in the dark for 60 min at 37°C. Then, the sections were incubated in 4, 6-diamidino-2-phenylindole (DAPI) at 37°C for 8 min. Next, they were washed with PBS and mounted with 50% glycerol.

## Statistical Analysis

The results are expressed as the means±SD from triplicate independent experiments and analyzed through *t*-test (two sided) using the Statistical Product and Service Solutions (SPSS) 17 software. A *p* value of less than 0.05 was considered to be statistically significant.

## Results

### Identification and Characterization of Exosomes

Exosomes derived from B16-F10 cells were identified by nanoparticle tracking analyzer (NTA), dynamic light scattering (DLS), Western blot (WB), and transmission electron microscopy (TEM). The effective size range of exosomes as determined by NTA were 70–520 nm with a mean particle size of  $169.7 \pm 4.62$  nm (Figure 1A). The most frequent events of exosomes as determined by DLS were around 185 nm (Figure 1B). We confirmed the presence of known melanoma exosome markers, including TSG101 and TYRP2 (Figure 1C). TEM was used to determine the morphology and size of the exosomes. Exosomes exhibit a variety of characteristics and features, and were of different sizes and shapes, though mostly spheroid (Figure 1D).

### In vitro Fusion of B16-F10 Exosomes with Fibroblasts

After co-cultured with CFSE-labeled exosomes, we observed a marked time-independent increase in the

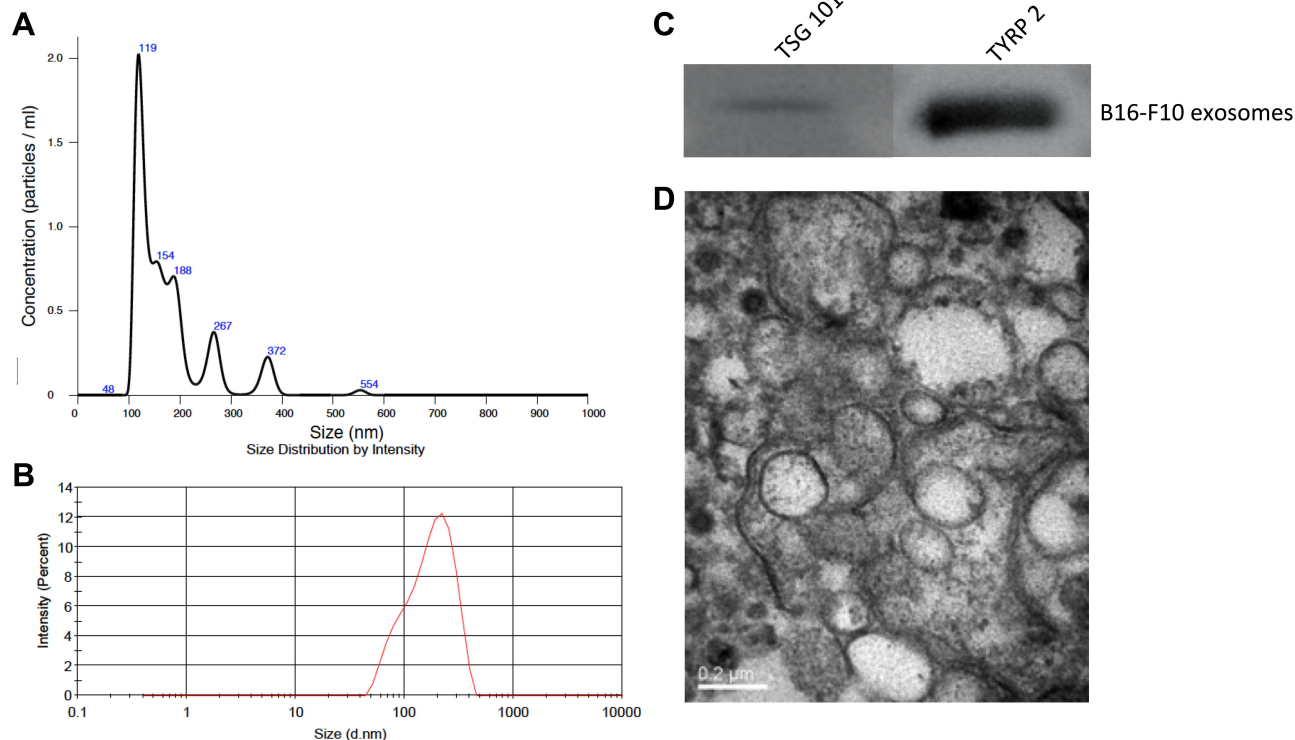


**Figure 1** The characteristics of exosomes determined by NTA, DLS, WB, and TEM. **(A)** Representative size frequency by NTA. **(B)** Size frequency of exosomes by DLS. **(C)** Representative western-blot of TYRP2 and TSG101 in exosomes isolated from B16-F10 cells. Glyceraldehyde-3-phosphate dehydrogenase (GAPDH) was used as a loading control (not shown). **(D)** A representative electron microscopic image of exosomes derived from B16-F10 cells.



fluorescence density of fibroblasts. When co-cultured with fibroblast cells, a time-dependent increase in exosomes density was observed in fibroblast cells, which gradually distributes to illuminate the outline of treated fibroblasts. Under the confocal microscope the green fluorescence of CFSE-labeled exosomes was observed in the fibroblast cells after co-culture with fibroblast cells for 6 hours. The CFSE-labeled exosomes could be seen in the fibroblast cells in the number of less. After co-culture for 12 h, a small portion of the fibroblast cells could initially be visualized by green fluorescence, then the fluorescence concentration in the cytoplasm appeared, indicating that CFSE-labeled exosomes were endocytosed by fibroblast cells. After co-culture for 24 h, green fluorescence was observed in almost all fibroblast cells. With increasing co-culture time, more and more fibroblast cells contained green fluorescence, indicating that the number of fibroblast cells endocytosing CFSE-labeled exosomes gradually

increased. Through 48 h of co-culture fibroblast cell uptake of CFSE-labeled exosomes is evident (Figure 2).

## Tumor Exosomes Alter Fibroblast Cell Invasive Potential

Exosome-treated fibroblast cell had greater invasive capability as compared to untreated fibroblast cells (Figure 3). Both groups of cells were cultured in the sustained growth state – cell indices increased during culture time. However, the curve of exosome-treated fibroblast cells begins to differ from the curve of untreated fibroblast cells after co-culture for 12h (Figure 3A). No difference in cell index was observed/witnessed between exosome-treated fibroblast cells and untreated fibroblast cells at 24h, but at 48h exosome-treated fibroblast cells had a significantly increased cell index compared to untreated fibroblast cells (Figure 3B). The pink curve (1.2g/L), blue curve (0.6g/L) and red curve (6.0g/L) was separated from the green curve (control group) and

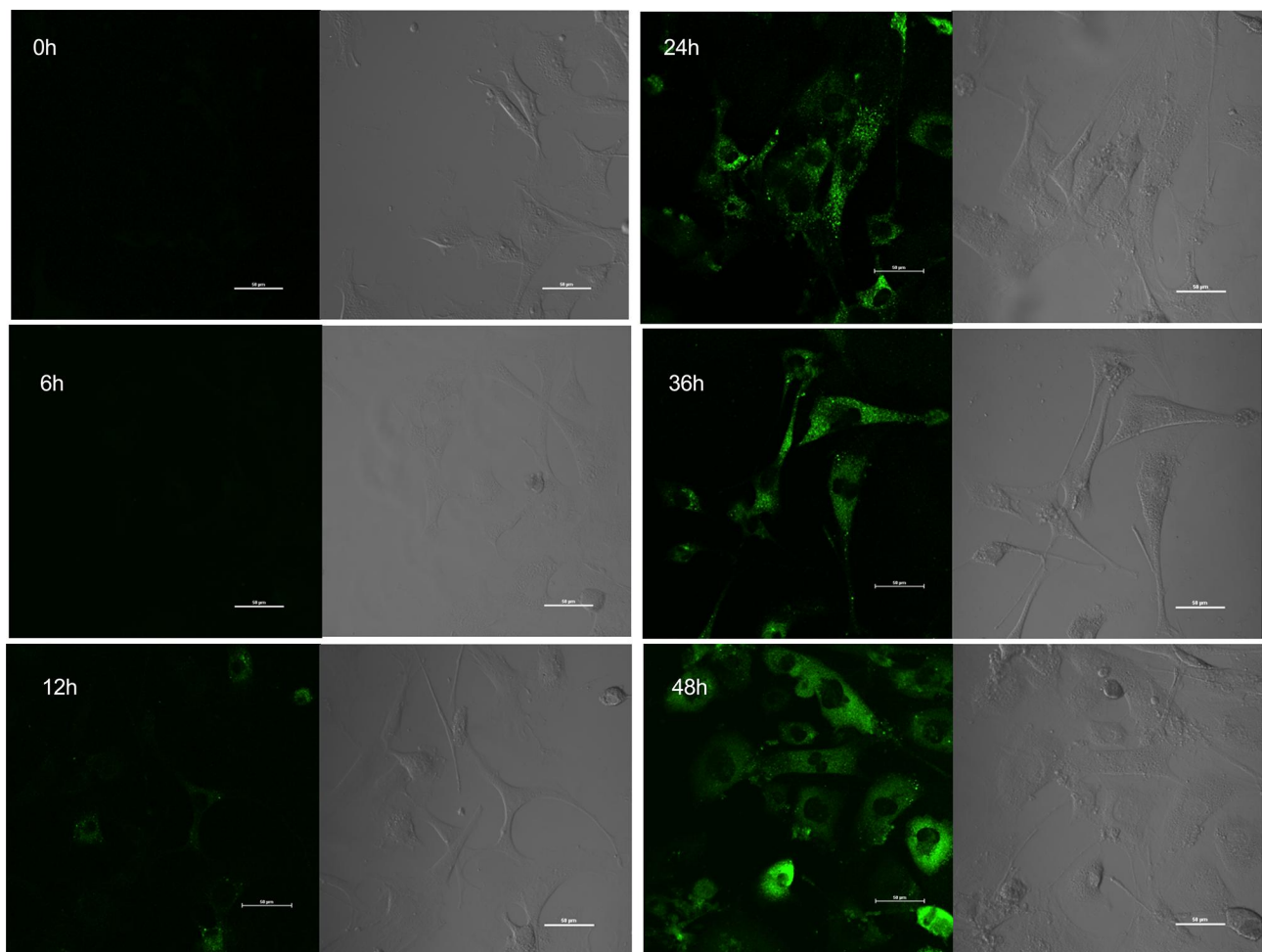


**Figure 2** Interaction between exosomes and fibroblasts. A time-dependent increase in exosomes density was observed in fibroblast cells, co-culture fibroblast cell uptake of CFSE-exosomes is evident after 48h. CFSE-labeled exosomes were observed under a confocal microscope. Scale bars, 50 µm.

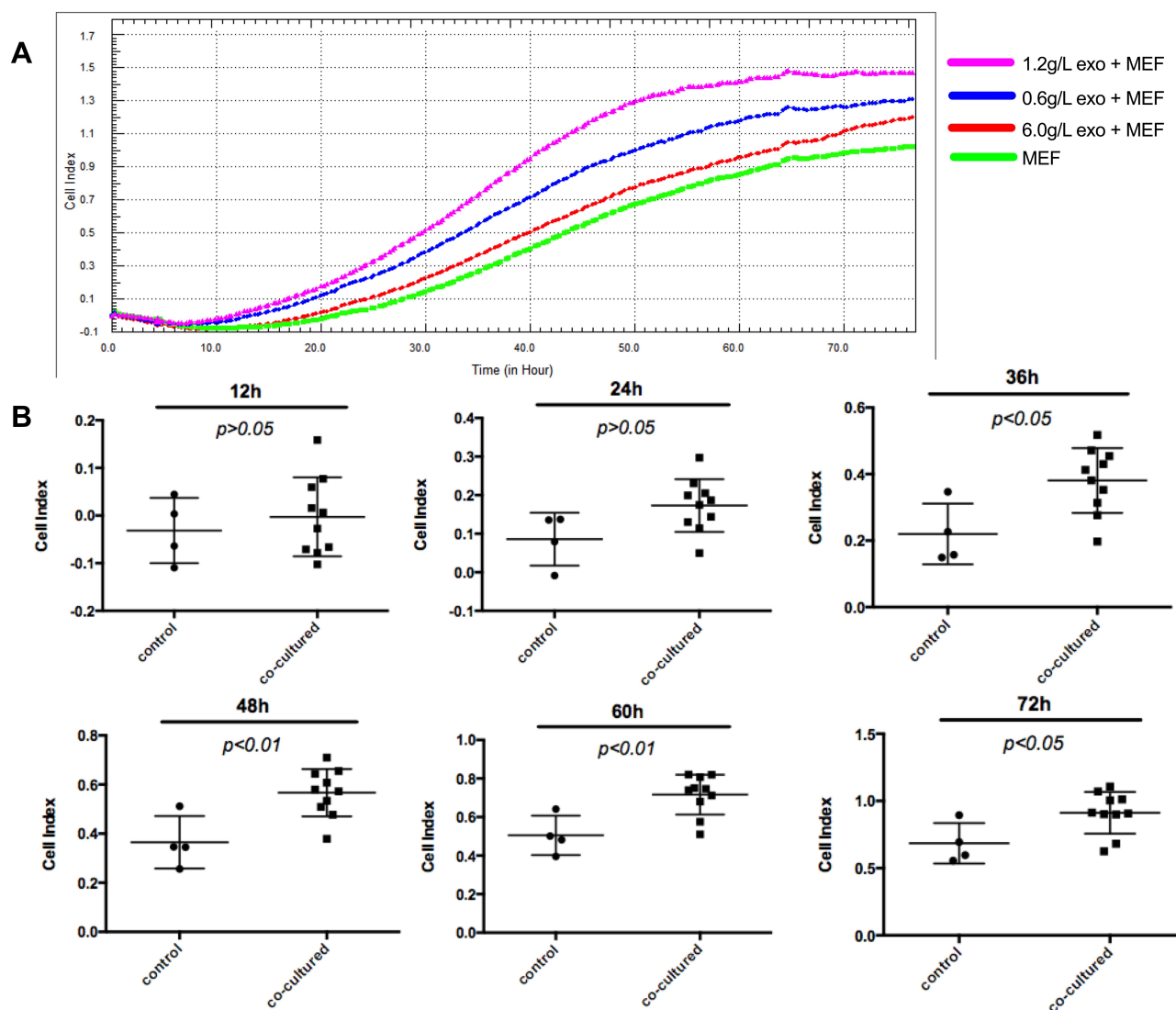


**Figure 3** Invasion of co-cultured fibroblast cells reported as variation of the normalized cell index (CI). The pink curve (1.2g/L), blue curve (0.6g/L) and red curve (6.0g/L) was separated from the green curve (control group) (A) and the cell index was higher than that of the control group (B).

the cell index was higher than that of the control group. The pink curve (1.2g/L) was the highest at co-cultured end (Figure 3A). Compared with the control group, the cell index of the pink group (1.2g/L) showed no significant difference between the two groups at 12 h and 24 h after co-culture. When the cells were co-cultured for 36 h, the invasiveness of the two groups were different. After 60 h, the invasiveness of the two groups were still significantly different until the end of co-cultured time (Figure 3B).

### miR-21 is Involved in the Invasiveness of Exosome-Treated Fibroblasts

Exosomes are known to promote the horizontal transfer of molecules to recipient cells. Our results show that exosomes

from highly malignant B16-F10 melanoma cells increase the invasive tendency of fibroblast cells (Figure 4). Given the key role of miR-21 signaling in the invasion phenotype, we focused our functional analyses on this oncogene. We hypothesized that exosomes could horizontally transfer miR-21 from melanoma cells to fibroblast cells and that this transfer could be a previously unknown mechanism for promoting invasive progression. Furthermore, miR-21 inhibitor is a sequence that can specifically bind to miR-21 to suppress its function. We first established the amounts of miR-21 in co-cultured group and inhibitor group after co-cultured for 48 h (Figure 4A). Fibroblast cells were exposed to B16-F10-derived exosomes and 48 h later miR-21 expression was increased in the fibroblast cells. This result indicates that the increase in miR-21

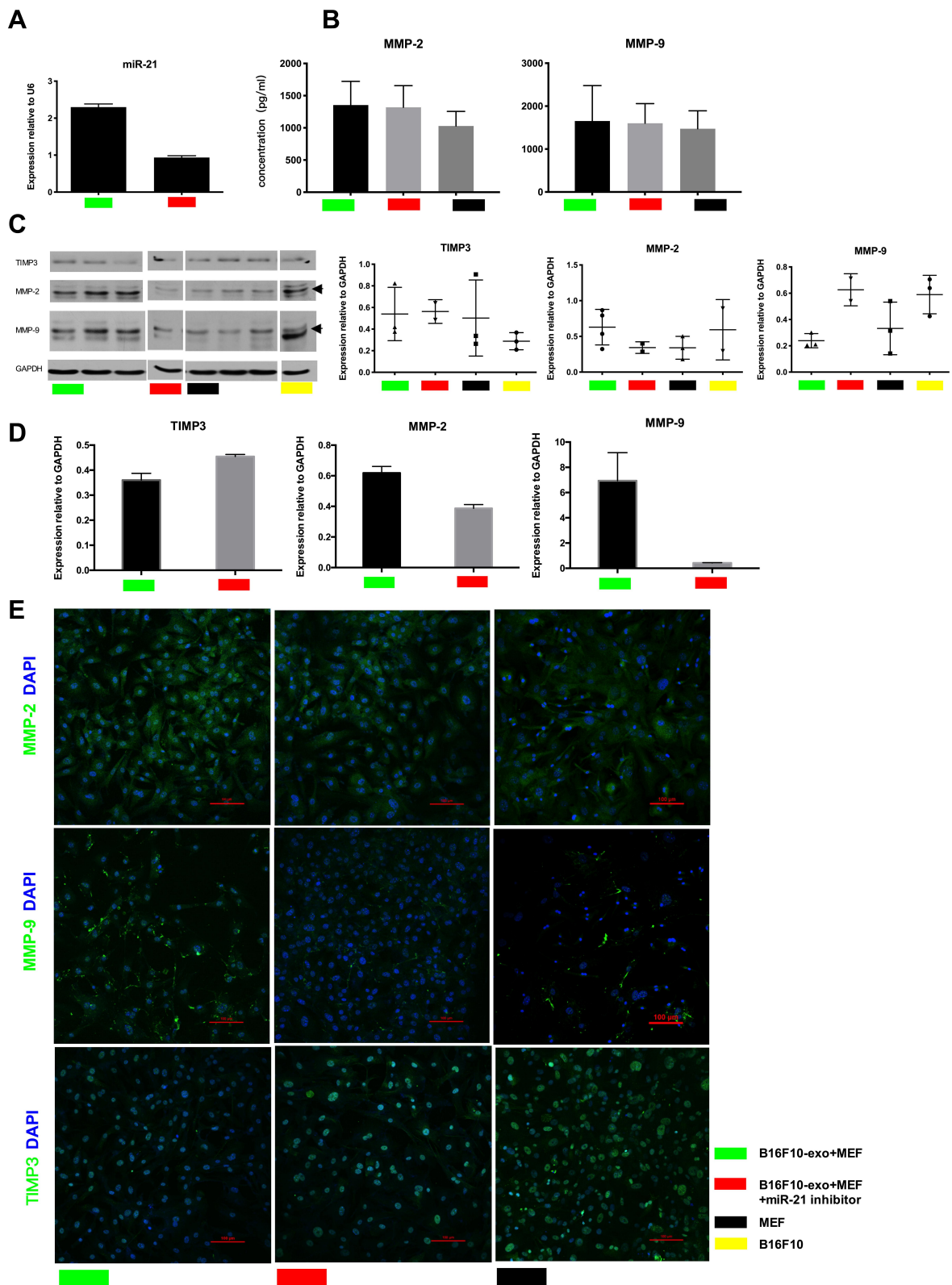


**Figure 4** Role of tumor-derived exosomes miR-21 in cell invasion. **(A)** miR-21 expression in different groups. **(B)** ELISA of MMP2, MMP9. **(C)** Representative Western blot of TIMP3, MMP2, MMP9. **(D)** Quantitative real-time PCR analysis of MMP2, MMP9, TIMP3. **(E)** Confocal microscope analysis of TIMP3, MMP2 and MMP9 distribution (green) of fibroblast cells after cultured 48 h. Scale bars, 100  $\mu$ m.

expression observed in fibroblasts is due to changes induced by miR-21 and not the result of exosome-mediated protein transfer between melanoma cells and fibroblasts. Moreover, the expression of MMP2 and MMP9 in the co-cultured group increased relative to the control group, while the expression of TIMP3 was decreased in the co-cultured group. Moreover, we detect the secretion level difference of MMP2, MMP9 in fibroblast cells cultured media and find that the secretion level of MMP2, MMP9 of co-culture group was higher than those of control. However, after miR-21 was inhibited, MMP2 and MMP9 expression weaker in the co-cultured group. The expression of TIMP3 in the miR-21-inhibited group was increased relative to the co-cultured group. Furthermore, compared to the co-culture group, the expression of MMP2 and MMP9 in fibroblast cells was significantly increased and the expression of TIMP3 was decreased in co-cultured fibroblast cells by western-blot analysis and qPCR. The secretion level of MMP2, MMP9 of inhibitor group was lower than those of co-culture group. These data suggest that exosome-mediated miR-21 transfer at least partially-mediates increased invasive ability of fibroblast cells.

## Discussion

Tumor cells release membrane nanofragments called tumor-derived exosomes that are believed to play an important role in cancer progression.<sup>16</sup> Recent studies suggest that exosomes within the tumor microenvironment are emerging as potent mediators for cell–cell communication.<sup>17</sup> Previously, it has been identified that melanoma cells exhibit increased invasive and metastatic characteristics after being cultured on feeder fibroblasts which were first treated with melanoma-derived exosomes.<sup>12</sup> However, only limited information was available regarding the effect of tumor exosomes on the phenotype of mesenchymal cells. We wanted to study the effect of tumor-derived exosomes on the fibroblast cells themselves, and to understand the impact on melanoma invasion and metastasis.

Here we observed that the particle size of exosomes is mainly distributed in the range of 70–520 nm (Figure 1B) and the mean particle size is  $169.7 \pm 4.62$  nm. Electron microscopy of exosomes demonstrated a bilayer membrane on the surface with 100 nm diameter and the presence of light-stained protein density inside, consistent with They et al.<sup>15</sup> Thus, the measured altitudes provide only a comparison of the relative size of objects. Due to their formation, exosomes share certain surface characteristics of protein expression with the source donor cell.<sup>17</sup> Here we found that melanoma exosomes express melanin-specific protein TYRP2 and exosome-specific protein TSG101.<sup>18</sup>

Endocytosis of exosomes is an essential part of signaling via exosomes. Zech<sup>19</sup> found that when the exosomes were in the receptor cell environment, exosomes would bind with the receptor cell surface and undergo endocytosis into the cells. In this study, confocal microscopy indicated that at 12 h of exposure a small amount of exosome-associated fluorescence was present in fibroblast cells, while at 24 h a large amount of exosome-associated fluorescence was present inside the cells. This means that different sizes of exosomes in the cell are indiscriminately introduced into the cell.

All of the above data suggest that tumor-derived exosomes alter the invasive potential of fibroblast cells. When assessing the uptake of B16-F10 cell-derived exosomes into fibroblast cells, fibroblast uptake of tumor-derived exosomes occurred in a time-dependent manner, like in the initial confocal fluorescent experiment. This suggests that the invasion of fibroblast cells would also occur in a time-dependent manner. We utilized an xCELLigence Real-time Cell Analyzer (RTCA) machine to observe real-time, quantitative changes in cell invasion by the cell-cell index. However, our results showed that the highest dose group is not the highest invasive ability probably due to excessive exosomes triggering some inhibition reaction. This suggests that the invasion of fibroblast cells would not occur in a dose-dependent manner. After 72 h of co-culture, we used RTCA to evaluate the invasive and metastatic tendencies of co-cultured cells. The results found that after exosome exposure fibroblast cells exhibited more invasive potential. When co-cultured for 36 h, the co-cultured cells had greater invasiveness than the control group, with the invasion ability of fibroblast cells increasing with time. The uptake of exosomes into fibroblast cells increased corresponding with the duration of co-culture time. Uptake of exosomes into fibroblast cells resulted in a shift in phenotype characterized by increased invasiveness. In addition to increased invasiveness, we also observed an increase in the metal-protease activity of fibroblast cells after co-culture. Matrix metalloproteinases (MMPs) are a group of zinc and calcium-dependent endopeptidases, the increased expression of which are closely related to the invasion and metastasis of tumors. MMPs are a family of structurally related zinc-dependent endopeptidases collectively capable of degrading essentially all components of the extracellular matrix (ECM), play a role in pathological conditions with excessive degradation of ECM, such as tumor invasion, and tumor metastasis.<sup>20–22</sup> MMP2-deficient mice show reduced angiogenesis and tumor progression and MMP9-deficient mice show impaired metastasis formation.<sup>23</sup> We also used different amounts of exosomes to co-culture with fibroblast



cells. Interestingly, we found that the amount of exosomes the fibroblast cells were cultured with was inversely correlated to the invasive effect on the fibroblast cells. This prompted us to question if perhaps an excess concentration of tumor-derived exosomes content may result in inhibiting a malignant phenotype. To this end, we performed a migration assay but found no significant difference. Previous studies have injected tumor-derived exosomes into mice, resulting in myeloid progenitor cells demonstrating a migratory phenotype that has malignant phenotype characteristics of tumors and promotes the formation of tumor microenvironment in tumor metastases.<sup>17</sup> We speculate that the exosomes of B16-F10 cells may contain the genetic information necessary to induce a phenotypic change in normal cells to become more malignant, but still not yet completely transformed into a malignant tumor. Fibroblast cells may be induced by exosomes of B16-F10 cells to become tumor-associated fibroblasts, which are more invasive and migratory than normal fibroblasts. It is possible that the co-cultured time studied is not long enough for complete malignant transformation to occur. We also demonstrated that fibroblast cells displayed some MMP2 protein expression in multiple assays, suggesting migration ability. In our data, fibroblast cells were also observed to have a migration force comparable to that of the induced cells.

MiR-21 was involved in the invasiveness of exosomes-treated fibroblasts. In our previous work, miRNA array of exosomes found that there was a large number of miRNA in melanoma exosomes and that miR-21 was overexpressed. MiR-21 is overexpressed in many tumors and has been linked to various cellular processes.<sup>10</sup> MiR-21 is highly expressed in melanoma cells and apparently plays a pivotal role in melanoma genesis.<sup>24</sup> In the study presented here, we have identified a new link between miR-21 and the metastatic behavior of melanoma cells. Compared with untreated cells, it was confirmed that exosomes derived from B16-F10 cells were rich in miR-21. Therefore, we hypothesized that exosomes could horizontally transfer miR-21 derived from melanoma cells to fibroblast cells. It has been suggested that TIMP3 is one of the miR-21-targeted genes. Furthermore, TIMP3 is an inhibitor of MMPs protein,<sup>25–27</sup> and some studies have shown that miR-21 can enhance the invasiveness of cells by inhibiting TIMP3 expression simultaneously. We hypothesize that exosomes inhibit the expression of TIMP3 by carrying overexpressed miR-21 so that the expression of MMPs protein is increased and the invasiveness of cells is enhanced. In our experiments, we identified that the expression of miR-21 in the co-cultured group was stronger than that in the control group. Meanwhile, we found that the expression of MMP2 and MMP9 was

significantly increased in the co-cultured group, which indicated that the ability of the cells to penetrate the matrix was enhanced and attributable to the secretion of MMP2 and MMP9. Future work will focus on a bioinformative approach to understanding the overall transfer of invasion-related information via miRNA in melanoma-derived exosomes.

## Conclusion

In conclusion, we found that miR-21 in B16-F10-derived exosomes induced a change in fibroblast cell phenotype to increased invasive tendency. Tumor-derived exosomes interact directly with normal cells serving as macro-messengers and molecular cargo transfer resulting in enhancement of tumor invasion. This in turn contributes to melanoma progression. A better understanding of the role of exosomes in tumor invasion may provide novel approaches to disrupt tumor invasion and progression. We believe that in addition to inducing surrounding tumor cells to release cytokines for the promotion of tumor invasion and metastasis, tumor cells can also alter the phenotype of surrounding cells by exosomes. Tumor expansion is not just the work of tumor cells themselves, and perhaps changes in the surrounding non-malignant cells contributes to tumor invasion as well. This may be a new mechanistic understanding of tumor cell invasion and provide novel insights for future therapies.

## Ethics Approval and Informed Consent

This work was conducted under the support of the Ethics Committee of Chongqing Medical University.

## Acknowledgments

We thank Dr. Zhou Daxue for helpful conversations, Dr. Xin Yu for assistance with the samples, and Dr. Dou Xiaoyun for producing several of the figures.

## Disclosure

The authors report no conflicts of interest in this work.

## References

1. Johnstone RM, Adam M, Hammond JR, Orr L, Turbide C. Vesicle formation during reticulocyte maturation. Association of plasma membrane activities with released vesicles (exosomes). *J Biol Chem.* 1987;262:9412–9420. doi:10.1557/PROC-0928-GG08-04
2. Théry C, Zitvogel L, Amigorena S, Théry C, Zitvogel L, Amigorena S. Exosomes: composition, biogenesis, and function. *Nat Rev Immunol.* 2002;2:569–579. doi:10.1038/nri855

3. Iero M, Valenti R, Huber V, et al. Tumour-released exosomes and their implications in cancer immunity. *Cell Death Differ.* 2008;15:80–88. doi:10.1038/sj.cdd.4402237
4. Skog J, Würdinger T, Van RS, et al. Glioblastoma microvesicles transport RNA and proteins that promote tumour growth and provide diagnostic biomarkers. *Nat Cell Biol.* 2008;10:1470–1476. doi:10.1038/ncb1800
5. Alnedawi K, Meehan B, Kerbel RS, Allison AC, Rak J. Endothelial expression of autocrine VEGF upon the uptake of tumor-derived microvesicles containing oncogenic EGFR. *Proc Natl Acad Sci U S A.* 2009;106:3794–3799. doi:10.1073/pnas.0804543106
6. Valenti R, Huber V, Iero M, Filipazzi P, Parmiani G, Rivoltini L. Tumor-released microvesicles as vehicles of immunosuppression. *Cancer Res.* 2007;67:2912–2915. doi:10.1158/0008-5472.CAN-07-0520
7. Valadi H, Ekström K, Bossios A, Sjöstrand M, Lee JJ, Lötvall JO. Exosome-mediated transfer of mRNAs and microRNAs is a novel mechanism of genetic exchange between cells. *Nat Cell Biol.* 2007;9:654–659. doi:10.1038/ncb1596
8. Calin GA, Croce CM. MicroRNA signatures in human cancers. *Nat Rev Cancer.* 2006;6:857–866. doi:10.1038/nrc1997
9. Bartel DP. MicroRNAs: genomics, biogenesis, mechanism, and function. *Cell.* 2004;116:281–297. doi:10.1016/S0092-8674(04)00045-5
10. Yang CH, Yue J, Pfeffer SR, Handorf CR, Pfeffer LM. MicroRNA miR-21 regulates the metastatic behavior of B16 melanoma cells. *J Biol Chem.* 2011;286:39172–39178. doi:10.1074/jbc.M111.285098
11. Se MDC, Latchana N, Levine KM, et al. MiR-21 enhances melanoma invasiveness via inhibition of tissue inhibitor of metalloproteinases 3 expression: in vivo effects of MiR-21 inhibitor. *PLoS One.* 2014;10:e0115919–e. doi:10.1371/journal.pone.0115919
12. Zhao XP, Wang M, Song Y, et al. Membrane microvesicles as mediators for melanoma-fibroblasts communication: roles of the VCAM-1/VLA-4 axis and the ERK1/2 signal pathway. *Cancer Lett.* 2015;360:125–133. doi:10.1016/j.canlet.2015.01.032
13. Lawrenson K, Grun B, Benjamin E, Jacobs JJ, Dafou D, Gayther SA. Senescent fibroblasts promote neoplastic transformation of partially transformed ovarian epithelial cells in a three-dimensional model of early stage ovarian cancer. *Neoplasia.* 2010;12:317–325. doi:10.1593/neo.91948
14. Pavlides S, Whitakermenezes D, Castelloccros R, et al. The reverse Warburg effect: aerobic glycolysis in cancer associated fibroblasts and the tumor stroma. *Cell Cycle.* 2009;8:3984–4001. doi:10.4161/cc.8.23.10238
15. Théry C, Amigorena S, Raposo G, Clayton A Isolation and characterization of exosomes from cell culture supernatants and biological fluids. *Curr Protoc Cell Biol.* 2006;4: 3.22.1–3.9. doi: 10.1002/0471143030.cb0322s30
16. Kharaziha P, Ceder S, Li Q, Panaretakis T. Tumor cell-derived exosomes: a message in a bottle. *Biochim Biophys Acta.* 2012;1826:103–111. doi:10.1016/j.bbcan.2012.03.006
17. Peinado H, Alečković M, Lavotshkin S, et al. Melanoma exosomes educate bone marrow progenitor cells toward a pro-metastatic phenotype through MET. *Nat Med.* 2012;18:883–891. doi:10.1038/nm.2753
18. Babst M, Odorizzi G, Estepa EJ, Emr SD. Mammalian tumor susceptibility gene 101 (TSG101) and the yeast homologue, Vps23p, both function in late endosomal trafficking. *Traffic.* 2000;1:248–258. doi:10.1034/j.1600-0854.2000.010307.x
19. Zech D, Rana S, Büchler MW, Zöller M. Tumor-exosomes and leukocyte activation: an ambivalent crosstalk. *Cell Communication Signaling.* 2012;10:4241–4247. doi:10.1186/1478-811X-10-37
20. Cawston T. Matrix metalloproteinases and TIMPs: properties and implications for the rheumatic diseases. *Mol Med Today.* 1998;4:130–137. doi:10.1016/S1357-4310(97)01192-1
21. Nagase HH, Woessner JF. Matrix metalloproteinases. *J Biol Chem.* 1999;274:21491–21494. doi:10.1074/jbc.274.31.21491
22. Westermarck J, Kähäri V. Regulation of matrix metalloproteinase expression in tumor invasion. *FASEB J.* 1999;13:781–792. doi:10.1016/j.ddmod.2011.06.001
23. Itoh T, Tanioka M, Yoshida H, Yoshioka T, Nishimoto H, Itohara S. Reduced angiogenesis and tumor progression in gelatinase A-deficient mice. *Cancer Res.* 1998;58(5):1048–1051.
24. Satzger I, Mattern A, Kuettler U. microRNA-21 is upregulated in malignant melanoma and influences apoptosis of melanocytic cells. *Exp Dermatol.* 2012;21:509–514. doi:10.1111/j.1600-0625.2012.01510.x
25. Wagner SN, Ockenfels HM, Wagner C, Soyer HP, Goos M. Differential expression of tissue inhibitor of metalloproteinases-2 by cutaneous squamous and basal cell carcinomas. *J Investigative Dermatol.* 1996;106:321–326. doi:10.1111/1523-1747.ep12342979
26. Airola K, Ahonen M, Johansson N. Human TIMP-3 is expressed during fetal development, hair growth cycle, and cancer progression. *J Histochem Cytochem.* 1998;46:437–447. doi:10.1177/002215549804600403
27. Sutinen M, Kainulainen T, Hurskainen T, et al. Expression of matrix metalloproteinases (MMP-1 and -2) and their inhibitors (TIMP-1, -2 and -3) in oral lichen planus, dysplasia, squamous cell carcinoma and lymph node metastasis. *Br J Cancer.* 1998;77:2239–2245. doi:10.1038/bjc.1998.372

## Cancer Management and Research

Dovepress

### Publish your work in this journal

Cancer Management and Research is an international, peer-reviewed open access journal focusing on cancer research and the optimal use of preventative and integrated treatment interventions to achieve improved outcomes, enhanced survival and quality of life for the cancer patient.

The manuscript management system is completely online and includes a very quick and fair peer-review system, which is all easy to use. Visit <http://www.dovepress.com/testimonials.php> to read real quotes from published authors.

Submit your manuscript here: <https://www.dovepress.com/cancer-management-and-research-journal>